Research Square

Preprints are preliminary reports that have not undergone peer review.
They should not be considered conclusive, used to inform clinical practice,
or referenced by the media as validated information.

Bdh1-Mediated βOHB Metabolism Ameliorates Diabetic Kidney Disease by Activation of Nrf2-Mediated Antioxidative Pathway

Sheng-rong Wan
The Affiliated Hospital of Southwest Medical University
Fang-yuan Teng
The Affiliated Hospital of Southwest Medical University
Wei Fan
The Affiliated Hospital of Southwest Medical University
Xin-yue Li
The Affiliated Hospital of Southwest Medical University
Bu-tuo Xu
The Affiliated Hospital of Southwest Medical University
Xiao-zhen Tan
The Affiliated Hospital of Southwest Medical University
Man Guo
The Affiliated Hospital of Southwest Medical University
Chen-lin Gao
The Affiliated Hospital of Southwest Medical University
Zong-zhe Jiang
The Affiliated Hospital of Southwest Medical University
Yong Xu (xywyll@swmu.edu.cn)
The Affiliated Hospital of Southwest Medical University https://orcid.org/0000-0002-9534-6252

Research Article

Keywords: βOHB, Bdh1, Diabetic Kidney Disease, Nrf2

Posted Date: October 21st, 2021

DOI: https://doi.org/10.21203/rs.3.rs-976505/v1

License: This work is licensed under a Creative Commons Attribution 4.0 International License.
Read Full License

Abstract

Ketogenic diet (KD) and β-Hydroxybutyrate (βOHB) has been widely reported as an effective therapy for metabolic diseases. β-hydroxybutyrate dehydrogenase 1 (Bdh1) is the rate-limiting enzyme of ketone metabolism. In this study, we investigated the Bdh1-mediated βOHB metabolic pathway in pathogenesis of diabetic kidney disease (DKD). Human renal tubule epithelial cells (HK-2 cells) induced by high glucose (HG) or palmitic acid (PA) were used to transfect with Bdh1 siRNA or plasmid-flag-Bdh1. Reactive oxygen species (ROS) levels, nuclear factor red 2-related factor 2 (Nrf2) protein expression, and βOHB-acetoacetate (AcAc)-succinate-fumarate metabolic flux were detected. Five-week-old C57 BKS db/db obese diabetic mice (db/db) and their littermate controls (+/+) were treated with KD, βOHB, and adeno-associated virus (AAV9)-Bdh1, respectively. Renal function was determined by urinary albumin/creatinine ratio (ACR), and histopathological, immunohistochemistry (IHC), TUNEL staining of kidney were also performed. The renal expression of Bdh1 was down-regulated in DKD mouse models, diabetic patients and HG or PA induced HK-2 cells. Bdh1 overexpression or βOHB treatment protected HK-2 cells from glucotoxicity and lipotoxicity by inhibiting ROS overproduction. Mechanistically, Bdh1-mediated βOHB metabolism activated Nrf2 through enhancement of metabolic flux composed of βOHB-acetoacetate-succinate-fumarate. Moreover, *in vivo* studies showed that AAV9-mediated Bdh1 renal expression successfully reversed the fibrosis, inflammation and apoptosis in kidneys from C57 BKS db/db mice. Notably, either βOHB supplementation or KD feeding could elevate the renal expression of Bdh1 and reverse the progression of DKD. Our results revealed a Bdh1-mediated molecular mechanism in pathogenesis of DKD and identified Bdh1 as a potential therapeutic target for DKD.

Introduction

Diabetes mellitus (DM) is a chronic and serious metabolic disease, which has a significant impact on patients and their families all over the world. The latest report of the international diabetes federation predicted that the number of people with diabetes in the world will reach 700 million at the year of 2045 [1]. As the most common microvascular complications of DM, diabetic kidney disease (DKD) is the main cause of chronic kidney disease (CKD) and end-stage renal disease (ESRD) [2–4]. Thus, studies aimed at clarifying the pathogenesis of DKD and exploring novel therapeutic targets to treat DKD are urgently needed.

Under the physiological conditions, the production and elimination of ROS reach a dynamic balance. The abnormal increase of ROS in diabetic patients leads to oxidative stress injury and inflammatory response, ultimately promotes the occurrence and development of DKD [5–7]. It is well known that the transcription factor Nrf2 can maintain intracellular redox homeostasis and reduce cell damage by regulating the expression of antioxidant proteins [8–10]. Xiao L et al. [11] found that the protective effect of mitoQ, a mitochondria-targeted antioxidant, on high glucose-treated HK-2 cells was partially blocked by Nrf2 knockdown. Fumarate, an intermediate product of the TCA cycle, is well known to activate Nrf2-mediated antioxidant response [12–14]. However, the role of metabolic regulation in Nrf2-mediated anti-ROS pathway and the pathogenesis of DKD is still unclear.

In the state of prolonged fasting, strenuous exercise or disease, fatty acids will produce ketone bodies in the liver through β-oxidation. Ketone bodies will be released into blood circulation and transported to extrahepatic organs such as the brain, heart and kidneys, where they are used as metabolic fuel for the tricarboxylic acid (TCA) cycle [15]. In the heart of diabetic patients, the intake of ketone bodies is increased and utilized as an energy source partially replacing glucose [16]. As a diet causing the elevation of endogenous ketone bodies, KD was first introduced by doctors as a therapeutic method of epilepsy [17] and then was reported to be beneficial for a variety of diseases, including diabetic cardiomyopathy and diabetic tractional retinal detachment[18–21]. In addition, KD intervention had been reported to show beneficial effect on T2DM and DKD [22–24]. Although an increasing number of evidence have been reported to support the relationship between KD and diseases, the underlying molecular mechanism is still unclear.

Ketone bodies is the sum of βOHB, acetoacetate (AcAc), and acetone. As the main component of ketone bodies, βOHB has been reported to be not only an alternative energy source for the body, but also mediates signal transduction in metabolic process to function in processes of antioxidant production, anti-inflammation and anti-aging [25, 26]. Bdh1 is the rate-limiting enzyme of ketone metabolism and can directly catalyze the metabolism of βOHB and promote the reciprocal transformation between βOHB and AcAc [25]. It has been reported that heart specific overexpression of Bdh1 can significantly ameliorate heart failure through inhibition of oxidative stress [27]. Moreover, up-regulation of Bdh1-mediated βOHB metabolism increases the concentration of fumarate, which subsequently activates Nrf2 to induce the expression of antioxidant stress response elements, and ultimately inhibit retinal degeneration under ischemic conditions [28]. However, the role of Bdh1-mediated βOHB metabolism in the pathogenesis of DKD is still unknown.

In this study, we report that Bdh1 deficiency is related to pathogenesis of DKD *in vivo* and glucotoxicity and lipotoxicity *in vitro.* We also demonstrate that Bdh1 functions as a previously unrecognized activator of Nrf2 through enhancement of metabolic flux composed of βOHB-AcAc-succinate-fumarate. Notably, the AAV-9 mediated renal expression of Bdh1 effectively relieved the progression of DKD and either βOHB supplementation or KD feeding could elevate the renal expression of Bdh1 and reverse the progression of DKD. Taken together, our findings suggest a promising new therapy for DKD via targeting Bdh1-mediated βOHB metabolism.

Materials And Methods

Animals

Five-week-old C57 BKS db/db male mice (n=20; 31.94±2.08g) and db/db littermate control (wild type, WT; n=5; 19.96±0.79g) mice were purchased from GemPharmatech Co., Ltd. (Nanjing, China). Animals were acclimatized before the experiments for at least one week, then they were randomly divided into seven groups (n=5 each). 60% high fat diet (HFD) and KD (74.2% fat, 8.9% protein, 3.2% carbohydrate) were purchased from Trophic Animal Feed High-Tech Co., Ltd. (Jiangsu, China). All animal experiments were

performed under the following condition: room temperature 23±1°C，relative humidity 60% ±10%, and an alternating 12h light-dark cycle in individually ventilated cages. Animal experiments were approved by the Institutional Animals Ethics Committees of Southwest Medical University and in accordance with the National Institutes of Health (NIH) guidelines for the care and use of laboratory animals.

Human renal samples

Samples from patients who had been diagnosed with diabetic nephropathy were collected from the Department of Pathology, The Affiliated Hospital of Southwest Medical University. Normal samples were collected from individuals who underwent tumor nephrectomies without diabetes or renal diseases. The study was conducted in accordance with the principles of the Declaration of Helsinki and was approved by the Research Ethics Committee of the Affiliated Hospital of Southwest Medical University after informing the patients.

Animal experiments

For AAV9-mediated Bdh1 renal expression, 100μL AAV9-Bdh1 (3.40E+12vg/mL, Beijing Syngentech Co., LTD. China) or the negative control (1.90E+13vg/mL) were injected into db/db mice *via* the caudal vein. In order to reduce the accidental death of mice, sodium β-hydroxybutyrate (Shanghai Macklin Biochemical Co., Ltd. China) was added by dissolving in drinking water as previously described [29] and supplied for db/db mice to drink freely. Body weight and blood glucose were recorded weekly.

HK-2 Cell culture

HK-2 cells (ATCC, USA) were cultured in low glucose Dulbecco's Modified Eagle Medium (DMEM, HyClone, Logan, Utah, USA) containing 10% fetal bovine serum (FBS, Sciencell, USA) and supplemented with 1% penicillin-streptomycin (PS, Beyotime, Shanghai, China). HK-2 cells were cultured at 37℃ with 5% CO2 until 60-70% confluence [30], cells were exposed to normal glucose (5.5 mM) as normal control (NC), HG (40mM), and PA (200μM, Sigma-Aldrich, Saint Louis, MO, USA) for 48h. PA was prepared as previously described [31].

Histopathological examination

The kidney tissues were fixed in 4% paraformaldehyde for 24h, embedded in paraffin and sectioned at 4-μm thickness. The sections were stained by the hematoxylin-eosin (H&E), or Masson-trichrome methods for light microscopic analysis and morphometry.

IHC staining

Briefly, 4-μm-thick paraffin sections were dewaxing hydration and stained with primary antibodies against Bdh1(1:100, ab193156, Abcam), IL-1β (1:100, #12242, Cell Signaling Technology). The sections were stained with biotin-labeled goat anti-rabbit IgG or biotin-labeled anti-mouse IgG and then treated with the

Horseradish enzyme labeled oopaltin of Streptomyces (Beijing ZSGB Biological Technology CO., LTD. China). Each photograph of the stained sections was scanned using a light microscope.

Immunofluorescence staining

Immunofluorescence (IF) staining for kidney paraffin sections and HK-2 cells were stained with anti-Bdh1 antibody (1:100) and Nrf2 (1:50, sc365949, Santa cruze). Cy3/FITC fluorescent dye-conjugated secondary antibody (1:200 dilution, Biosynthesis Biotech, China) were incubated for 60 min at room temperature in the dark. Nucleus was labeled with DAPI, and images were taken with a fluorescence microscope (Leica, Germany).

ROS and TUNEL assay

The level of ROS in HK-2 cells were measured by DCFH-DA fluorescent probe according to the ROS Assay Kit protocol (Beyotime, China). TUNEL staining for the kidney paraffin sections was performed according to the TUNEL Kit protocol (Roche, USA).

Human Bdh1 cDNA transfection

The human Bdh1-overexpressed plasmid (pCMV3-Bdh1-Flag) and the vector plasmid (pCMV3) were purchased from Beijing Sino Biological Inc. China and transfected into HK-2 cells with Lipofectamine 3000 (Invitrogen).

siRNA transfection

The siRNAs for Bdh1 and normal control (NC) were purchased from RiboBio (Guangzhou, China). The siRNA sequence of human Bdh1 gene was: 5′-GCCTAAACAGTGACCGATT-3′. The Bdh1 and NC siRNA were transfected into HK-2 cells with ribo*FECT*^{TM} CP Reagent and ribo*FECT*^{TM} CP Buffer (RiboBio, Guangzhou, China).

Measurement of AcAc, succinate and fumarate

The AcAc content in HK-2 cells was measured by human acetoacetate ELISA Kit (JL15388, Shanghai J&L Biological, China). The succinate and fumarate content of HK-2 cells were measured using the Succinate Assay Kit (MAK335, Sigma-Aldrich) and the Fumarate Assay Kit (MAK060, Sigma-Aldrich) according to the manufacturer's instructions.

qRT-PCR analysis

Total RNAs of renal tissue and HK-2 cells were extracted with the Trizol (Invitrogen). The ReverTra Ace qPCR RT Master Mix (FSQ-201, TOYOBO) was used for reverse transcription reaction and QuantiNova SYBR Green PCR Kit (QIAGEN, German) was used for qRT-PCR. The qRT-PCR was performed with Analytikjena qTOWER 3G real-time PCR system (JENA, German) according to the manufacturer's instructions. All primers used in this study were shown in Table S1. β-actin was used as an internal

reference gene to normalize target gene expression. All the samples were used in triplicates. The $2^{-\triangle\triangle Ct}$ method [32] was used to calculate the relative gene expression in comparison with the reference gene.

Western Blot analysis

Total proteins of mice renal and HK-2 cells were extracted with extraction buffer (RIPA). Nuclear proteins were extracted with Nucleoprotein Extraction Kit protocol (Shanghai Sangon Biotech, China). The protein samples were separated by sodium dodecyl sulfate-polyacrylamide gel electrophoresis (SDS-PAGE) and transferred into a PVDF membrane (Millipore). The membranes were incubated with 5% BSA to block other contaminants, and then with primary antibodies. Immunoblotting was performed using anti-Bdh1 antibody (1:1000 dilution), anti-Nrf2 antibody (1:500 dilution), anti-IL-1β antibody (1:1000 dilution), anti-β-actin antibody (1:4000 dilution, Beyotime, China), anti-Tubulin antibody (1:4000 dilution, Beyotime, China), anti-Histone H3 antibody (1:1000, Beyotime, China) and anti-flag antibody (1:1000, Beyotime, China).

Statistical Analysis

Data are expressed as the means ± standard deviation (SD) from triplicate experiments. Comparisons among groups were analyzed using one-way ANOVA analysis followed by 2-tailed unpaired Student's t-test using GraphPad Prism9. Differences were evaluated using $P<0.05$ was considered statistically significant. The statistical significance was *$p<0.05$, **$0.001<p<0.01$; ***$P<0.001$.

Results

RNA-seq analysis revealed Bdh1 reduction in DKD mouse model

As a major microvascular complication in diabetic patients, DKD is the leading cause of CKD and ESRD [2-4]. To gain a comprehensive understanding of potential DKD regulators, we performed an RNA-seq analysis comparing gene expression in the kidneys from db/db mice or WT mice after the db/db mice emerged obvious pathological features of DKD (Fig.1A). KEGG analysis showed that the "Synthesis and degradation of ketone bodies" pathway was significantly down-regulated (Fig.1B-C). Given that the KD was reported as an effective treatment for diabetes [33, 34], we supposed that the down regulation of "Synthesis and degradation of ketone bodies" pathway participates the pathogenesis of DKD. Consistently, qRT-PCR analysis confirmed the expression changes of Bdh1, Oxct1, Acat1, and Hmgcs1 (Fig.1D). Notably, among these four pathway members, Bdh1 has been reported to protect heart from heart failure in TCA mouse model. Thus, to identify whether Bdh1 is involved in DKD pathogenesis, we further detected the protein level of Bdh1. As shown in Fig.1E, protein level of Bdh1 in kidneys of db/db mice was significantly lower than that in kidneys of WT mice. Moreover, the decrease in Bdh1 expression was also confirmed by immunohistochemistry (IHC) and immunofluorescence (IF) analysis (Fig.1F). Consistent with the DKD mouse model, we also observed downregulation of Bdh1 in renal tissues of diabetic patients with kidney disease by IHC and IF staining (Fig.1G). These results indicates that the decrease of Bdh1 expression is related to the pathogenesis of DKD.

Bdh1 deficiency mediated high glucose (HG) or palmitic acid (PA)-induced ROS overproduction and inflammation

As it is known, hyperglycemia and hyperlipidemia are the two most obvious characteristics of type 2 diabetes [35]. In view of this, we established HG-induced glucotoxicity and PA-induced lipidtoxicity cell model with HK-2 cells to evaluate the effect of HG or PA on the Bdh1 expression. As expected, either mRNA level or protein level of Bdh1 was obviously reduced by HG or PA treatment in HK2 cells (Fig.2A-C), which was also identified by IF analysis (Fig.2D-E).

To investigate whether the Bdh1 reduction contribute to HG or PA-induced cell injury, we performed Bdh1 knockdown in HK2 cells (Fig.2F). Given that the increased ROS plays a central and prominent role in the pathogenesis of diabetic microvascular complications including DKD [36] and the overproduction of ROS was related to inflammation [37], we next detected the ROS level and observed significant increase of ROS in HK2 cells transfected with Bdh1 siRNA (Fig.2G). In addition, the protein level of activated proinflammatory factor, cleaved IL-1β, was also elevated by Bdh1 knockdown (Fig.2H), as well as the secretory IL-1β and IL-18 (Fig.2I-J). Collectively, these results suggest that Bdh1 deficiency might mediated HG or PA-induced cell injury by loss of anti-ROS function.

Either Bdh1 overexpression or βOHB supplementation reversed HG or PA-induced ROS overproduction and inflammation

As the Bdh1 deficiency led to increased ROS and inflammation, we next sought to determine whether HG or PA-induced Bdh1 reduction mediates HG or PA-induced cell injury. To this end, we transfected HK2 cells with flag-Bdh1 overexpression plasmid to block the HG or PA-induced Bdh1 reduction (Fig.3A). Notably, ROS assay showed that the Bdh1 overexpression significantly reduced the HG-induced ROS overproduction (Fig.3B, upper panels). Especially in PA-treated cells, Bdh1 overexpression nearly completely reversed the PA-induced ROS overproduction (Fig.3B, lower panels). As to inflammation, Bdh1 overexpression also reversed the HG or PA-induced activation of IL-1β (Fig.3C) and the increase of secretory IL-1β and IL-18 (Fig.3D-E). These evidences suggests that Bdh1 may play a protective role in DKD pathogenesis and pathological hyperglycemia and hyperlipidemia-induced Bdh1 reduction might mediate cell injury.

Given that Bdh1 is a key enzyme which mainly catalyzes the first step of βOHB metabolism, we next sought to determine whether βOHB supplementation could also exhibit protective effect on HG or PA-treated HK2 cells. In line with Bdh1 overexpression, βOHB supplementation also markedly reversed HG or PA-induced ROS overproduction (Fig.4A). Similarly, βOHB supplementation also reversed the HG or PA-induced activation of IL-1β (Fig.4B) and the increase of secretory IL-1β and IL-18 (Fig.4C-D). Taken together, these findings suggest that Bdh1 mediated βOHB metabolism play important role in protection of HG or PA-induced cell injury.

Bdh1-mediated βOHB metabolism promoted Nrf-2 nuclear translocation through the AcAc-succinate-fumarate metabolic pathway

Given that Nrf2 is a well-known transcription factor that regulates transcriptional induction of ARE-containing genes encoding antioxidant enzymes in response to cellular stresses including ROS [8-10], we next sought to determine whether Bdh1 mediates anti-ROS function through activation of Nrf2. As Nrf2 is a nuclear transcription factor, we detected the protein level of Nrf2 by western blot (WB) in nuclear extracts. Of note, in HK2 cells transfected with Bdh1 siRNA, Nrf2 protein level was significantly lower than that in cells transfected with control siRNA (Fig.5A). Moreover, either HG or PA could induce Nrf2 reduction in nuclear, whereas Bdh1 overexpression could reversed both HG and PA-induced Nrf2 reduction (Fig.5B). Consistent with the observations made in Bdh1 overexpression, βOHB supplementation also reversed both HG and PA-induced Nrf2 reduction in nuclear extracts (Fig.5C), which was further confirmed by Nrf2 nuclear translocation assay with immunostaining (Fig.5D). These data indicate that Bdh1-mediated βOHB metabolism promotes Nrf-2 nuclear translocation.

In Bdh1-mediated βOHB metabolism pathway, Bdh1 firstly metabolites βOHB into AcAc, which could enter into TCA cycle and then is metabolized into succinate and fumarate in turn (Fig.6A). As the fumarate is a well-known activator of Nrf2 signaling, we next investigated whether Bdh1 activated Nrf2 by increase of fumarate. Interestingly, we found that the concentrations of AcAc, succinate and fumarate were all decreased in HK2 cells transfected with Bdh1 siRNA (Fig.6B). Similarly, to that observed in Bdh1 siRNA transfected HK2 cells, both HG and PA treatment could reduce the levels of AcAc, succinate and fumarate, which was successfully blocked by Bdh1 overexpression (Fig.6C-D). Likewise, βOHB supplementation also reversed HG or PA-induced reduction of AcAc, succinate and fumarate (Fig.6E-F). These findings collectively reveal a metabolic flux composed of βOHB-AcAc-succinate-fumarate, which could be regulated by Bdh1 or βOHB and affected the downstream Nrf2 signaling (Fig.6G).

AAV9-mediated Bdh1 renal expression alleviated the progression of DKD

On the basis of the pronounced capacity of Bdh1 to inhibit ROS overproduction and inflammation, we next explored the therapeutic efficacy of Bdh1 expression in db/db mice. The experimental strategy is shown in Fig.7A. At the time point of 11 weeks after injection of the control or Bdh1-encoding virus, we performed ACR assay, which is the most important function indicator of kidney. Notably, although the Bdh1 renal expression didn’t affect the body weight and fasted blood glucose (Fig.S1A-B), we observed significantly lower ACR in AAV9-Bdh1-injected mice than that in the AAV9-Control-injected mice (Fig.7B). To confirm whether mouse Bdh1 was effectively expressed in the kidney using AAV9 vector, we detected the fluorescence intensity of GFP, which was co-expressed with Bdh1. We found that AAV9 encoding mouse Bdh1 was successfully delivered to the kidneys after 4 weeks of injection (Fig.7C). As expected, we observed increased Bdh1 expression in kidneys from AAV9-Bdh1 injected mice than that in AAV9-control injected mice (Fig.7D). In further histological analysis, AAV9-Bdh1 injected db/db mice showed normal morphology of glomerulus, unlike the glomerular hypertrophy in AAV9-control injected mice (Fig.7E). In addition, the DKD pathology-related fibrosis, inflammation and apoptosis were also substantially reduced by AAV9-Bdh1 injection (Fig.7E-G). These findings collectively provide strong support for the promising application of Bdh1 as a therapeutic target in DKD.

βOHB supplementation alleviated the progression of DKD

As βOHB supplementation showed similar effect to Bdh1 overexpression on HG or PA-induced ROS overproduction and inflammation in HK2 cells, we next sought to determine whether βOHB supplementation could ameliorate DKD. The experimental strategy is shown in Fig.8A. At the time point of 6 weeks after supplementation of βOHB by drinking water, we detected the serum level of βOHB and observed increased serum level of βOHB in db/db mice supplied with βOHB (Fig.8B). After that, we performed ACR assay. Although the βOHB supplementation didn't affect the body weight and fasted blood glucose (Fig.S1C-D), we found that there was significantly lower ACR in db/db mice supplied with βOHB than that with vehicle (Fig.8C). Moreover, the serum level of βOHB was negatively correlated with the value of ACR, indicating a strong ACR reduction capability of βOHB in DKD (Fig.8D). Interestingly, we also observed increased Bdh1 expression in kidneys from db/db mice supplied with βOHB (Fig.8E). In further histological analysis, db/db mice supplied with βOHB showed normal morphology of glomerulus, unlike the glomerular hypertrophy observed in db/db mice supplied with vehicle (Fig.8F). Consistent with AAV9-mediated Bdh1 renal expression, the DKD pathology-related fibrosis, inflammation and apoptosis were also substantially reduced by βOHB supplementation (Fig.8G-H). These results indicate that βOHB supplementation might ameliorate DKD by increasing renal expression of Bdh1, which finally promotes the βOHB metabolism.

Ketogenic diet alleviated the progression of DKD

The KD has been widely used in clinical studies and reported to have an anti-diabetic effect, while the underlying mechanisms have not been fully demonstrated. Given that the major production of KD is βOHB and Bdh1-mediated βOHB metabolism plays protective role in DKD, we next sought to determine whether KD could ameliorate DKD and whether it functions through Bdh1-mediated βOHB metabolism pathway. As shown in Fig.9A, WT or db/db mice were subjected to a standard diet (SD) or KD for 9 weeks, starting at the age of 8 weeks. Although the KD feeding didn't affect the body weight (Fig.S1E), the fasted glucose was reversed into normal level in KD-fed db/db mice (Fig.S1F). Compared with SD-fed db/db mice, db/db mice fed with KD showed increased blood level of βOHB (Fig.9B). Notably, KD treatment nearly completely reversed the increase of ACR in SD-fed db/db mice (Fig.9C). Interestingly, we observed increased Bdh1 expression again in kidneys from db/db mice fed with KD (Fig.9D). In further histological analysis, db/db mice fed with KD showed significantly pathological remission in kidneys, including fibrosis, inflammation and apoptosis (Fig.9E-G). These results indicate that feeding KD might ameliorate DKD by increasing blood βOHB and renal expression of Bdh1, which finally promotes the βOHB metabolism.

Discussion

In this study, we identified Bdh1 in renal cells as a potential therapeutic target for DKD. Our studies showed that expression of Bdh1 was reduced in DKD and HG or PA-treated HK-2 cells. Bdh1 overexpression or βOHB treatment can protect HK-2 cells from glucotoxicity and lipotoxicity.

Mechanistically, we found that Bdh1-mediated βOHB metabolism inhibits oxidative stress by activation of Nrf2 through upregulation of fumarate production. Of note, AAV9-mediated Bdh1 renal expression, βOHB supplementation or KD feeding can respectively reversed the fibrosis, inflammation and apoptosis in DKD. Thus, Bdh1-mediated βOHB metabolism in kidney lights a new way for DKD treatment.

In kidney, proximal renal tubular epithelial cells have reabsorption function and play an important role in the pathogenesis of DKD. However, the molecular mechanism by which tubular epithelial cells contribute to DKD is unclear. Of note, we found that the expression level of Bdh1 in HK-2 cells was much higher than that in Mpc5 cells (podocyte cell line) and SV40-MES cells (glomerular mesangial cell line) (date not shown). Our studies demonstrate a renal tubular Bdh1-mediated mechanism which participates in progression of DKD.

In the pathophysiology of diabetic kidney disease, increased oxidant species have been identified as the single unifying upstream event which holds a central and prominent role in progression of DKD [38]. Nrf2, a master positive regulator for genes related to antioxidant effects, is negatively regulated by kelch like epichlorohydrin associated protein 1 (Keap1) [39]. Thus, clinical trials of Keap1 inhibitors or Nrf2 inducers were conducted for treating DKD [40]. In addition, fumarate is well known to inhibit the binding of Keap1 to Nrf2 by modifying the cysteine residues [12, 26]. In this study, we identified Bdh1 as another Nrf2 activator in progression of DKD. We showed that Bdh1 overexpression upregulated the fumarate level by promoting metabolic flux composed of βOHB-AcAc-succinate-fumarate (Fig. 6). Moreover, Bdh1 also has been reported to play protective role in pressure overload-induced heart failure, whereas the underlying mechanism is unknown [27]. Our study indicates that the molecular mechanism by which Bdh1 functions protective effect in DKD might also contribute to the protective effect of Bdh1 in heart.

In recent years, gene therapy has emerged as a novel therapeutic modality that has the potential to cure substantial disease. As one of the gene deliveries vectors, AAV has achieved preclinical and clinical success in the treatment of human diseases by gene replacement, gene silencing and gene editing, which has been identified as a safe, well tolerated and effective therapeutic vector [41]. The US Food and Drug Administration recently approved AAV-based gene therapy for infant GM1 ganglioside storage disease and frontotemporal lobe dementia caused by granule protein mutation [42]. However, there is no evidence on AAV-based gene therapy of DKD. In this study, we successfully observed the renal expression of GFP by AAV9-GFP intravenous injection, indicating that AAV9 is an effective gene delivery tool for kidney target in mice (Fig. 7). Moreover, AAV9 mediated Bdh1 renal expression significantly inhibited the progression of DKD in db/db mice. Although the AAV9 is not a kidney-specific vector and the renal delivery is not so efficient as heart and liver [43], the effective amelioration of DKD which was observed in AAV9-Bdh1-injected db/db mice strongly suggests the AAV9 mediated gene targeting therapy as a promising treatment.

Ketone bodies metabolism refers to the processes of production in the liver (ketogenesis) and utilization in extrahepatic organs (ketolysis) [25]. KD is a diet with high fat and low carbohydrate, which can simulate the fasting metabolism and make the body in a state of ketogenesis [34]. However, the roles of

ketone bodies or KD in various disease are not so much clear and even contradictory. In one hand, βOHB and KD are clinically beneficial in several common human neurodegenerative diseases [26] and are reported to ameliorate hyperglycemia, mitochondrial dysfunction and cardiomyopathy in db/db mice [18]. KD was reported to reverse diabetic kidney disease in T1DM and T2DM mouse model as early as 2011 [24], which is consistent with our data (Fig. 9), but the underlying mechanism is still unknown. In the other hand, increased ketone bodies were reported to promote DKD progression in diabetic patients in another clinical study[44]. KD feeding promotes liver fibrosis and leads to liver damage in a T2DM mouse model [45]. In addition, KD-induced high protein intake may accelerate the progression of individual's kidney disease [46]. In this study, we showed that either βOHB supplementation or KD feeding could alleviate the progression of renal fibrosis, inflammation and apoptosis in db/db mice (Fig. 9). Of note, either βOHB supplementation or KD feeding elevated the renal expression of Bdh1, which functions as a strong antioxidant by activation of Nrf2. Our study further confirmed the protective effect of βOHB and KD on DKD and a Bdh1-mediated mechanism. Collectively, as coins have both sides, βOHB and KD might have unknown side effects when they protecting individuals from disease, which further suggests the Bdh1-targeted therapy as a more appropriate selection.

Taken together, our results provide evidence for the proposed mechanism depicted in Fig. 10. Hyperglycemia and hyperlipidemia in db/db mice lead to down-regulated expression of Bdh1, which subsequently down-regulates the fumarate level by metabolic flux composed of βOHB-AcAc-succinate-fumarate. The fumarate reduction decreases nuclear translocalization of Nrf2, a key inhibitor of ROS. The overproduction of ROS finally activates the DKD-related inflammation, fibrosis and apoptosis in kidney. Our findings also highlight the possibility of Bdh1 renal expression, βOHB supplementation and KD in attenuating DKD.

Abbreviations

DKD: diabetic kidney disease; DM: diabetes mellitus; CKD: chronic kidney disease; ESRD: end-stage renal disease; KD: ketogenic diet; TCA: tricarboxylic acid; βOHB: β-Hydroxybutyrate; Bdh1: β-hydroxybutyrate dehydrogenase 1; HG: high glucose; PA: palmitic acid; ROS: reactive oxygen species; Nrf2: nuclear factor red 2-related factor 2; AcAc: acetoacetate; AAV: adeno-associated virus; H&E: hematoxylin-eosin; IHC: immunohistochemistry; IF: immunofluorescence; qRT-PCR: quantitative real-time PCR; WB: western blot; ACR: albumin/creatinine ratio.

Declarations

Acknowledgements

This study was supported by the Project Program of Sichuan Clinical Research Center for Nephropathy (NO.2019YFS0537), the Sichuan Science and Technology Program (NO.2020YFS0456), the Natural Science Foundation of China (NO.81970676) and the Doctoral Research Initiation Fund of Affiliated Hospital of Southwest Medical University.

Author contributions

YX, ZZJ, SRW and FYT formulated the research question and study design. YX, ZZJ, SRW, FYT, WF, XYL, BTX, XZT, MG and CLG contributed towards the acquisition, analysis, or interpretation of data for the manuscript. All authors were responsible for drafting the article and revising it critically for important intellectual content. All authors approved submission.

Compliance with ethical standards

Conflict of interest All the authors declare that there is no duality of interest associated with this manuscript.

Data availability

The data that support the findings of this study are available from the corresponding author upon reasonable request.

References

1. Saeedi P, Petersohn I, Salpea P, Malanda B, Karuranga S, Unwin N et al (2019) Global and regional diabetes prevalence estimates for 2019 and projections for 2030 and 2045: Results from the International Diabetes Federation Diabetes Atlas, 9(th) edition. Diabetes Res Clin Pract 157:107843
2. Reidy K, Kang HM, Hostetter T, Susztak K (2014) Molecular mechanisms of diabetic kidney disease. J Clin Invest 124(6):2333–2340
3. Kanwar YS, Sun L, Xie P, Liu FY, Chen S (2011) A glimpse of various pathogenetic mechanisms of diabetic nephropathy. Annu Rev Pathol 6:395–423
4. Selby NM, Taal MW (2020) An updated overview of diabetic nephropathy: Diagnosis, prognosis, treatment goals and latest guidelines. Diabetes Obes Metab 22(Suppl 1):3–15
5. Niemann B, Rohrbach S, Miller MR, Newby DE, Fuster V, Kovacic JC (2017) Oxidative Stress and Cardiovascular Risk: Obesity, Diabetes, Smoking, and Pollution: Part 3 of a 3-Part Series. J Am Coll Cardiol 70(2):230–251
6. Lushchak VI (2014) Free radicals, reactive oxygen species, oxidative stress and its classification. Chem Biol Interact 224:164–175
7. Schieber M, Chandel NS (2014) ROS function in redox signaling and oxidative stress. Curr Biol 24(10):R453–R462
8. Schmidt HH, Stocker R, Vollbracht C, Paulsen G, Riley D, Daiber A et al (2015) Antioxidants in Translational Medicine. Antioxid Redox Signal 23(14):1130–1143
9. Casas AI, Dao VT, Daiber A, Maghzal GJ, Di Lisa F, Kaludercic N et al (2015) Reactive Oxygen-Related Diseases: Therapeutic Targets and Emerging Clinical Indications. Antioxid Redox Signal 23(14):1171–1185

10. Hejazian SM, Hosseiniyan Khatibi SM, Barzegari A, Pavon-Djavid G, Razi Soofiyani S, Hassannejhad S et al (2021) Nrf-2 as a therapeutic target in acute kidney injury. Life Sci 264:118581
11. Xiao L, Xu X, Zhang F, Wang M, Xu Y, Tang D et al (2017) The mitochondria-targeted antioxidant MitoQ ameliorated tubular injury mediated by mitophagy in diabetic kidney disease via Nrf2/PINK1. Redox Biol 11:297–311
12. Adam J, Hatipoglu E, O'Flaherty L, Ternette N, Sahgal N, Lockstone H et al (2011) Renal cyst formation in Fh1-deficient mice is independent of the Hif/Phd pathway: roles for fumarate in KEAP1 succination and Nrf2 signaling. Cancer Cell 20(4):524–537
13. Akino N, Wada-Hiraike O, Terao H, Honjoh H, Isono W, Fu H et al (2018) Activation of Nrf2 might reduce oxidative stress in human granulosa cells. Mol Cell Endocrinol 470:96–104
14. Linker RA, Lee D-H, Ryan S, van Dam AM, Conrad R, Bista P et al (2011) Fumaric acid esters exert neuroprotective effects in neuroinflammation via activation of the Nrf2 antioxidant pathway. Brain 134(3):678–692
15. Newman JC, Verdin E (2017) beta-Hydroxybutyrate: A Signaling Metabolite. Annu Rev Nutr 37:51–76
16. Mizuno Y, Harada E, Nakagawa H, Morikawa Y, Shono M, Kugimiya F et al (2017) The diabetic heart utilizes ketone bodies as an energy source. Metabolism 77:65–72
17. Wheless JW (2008) History of the ketogenic diet. Epilepsia 49(Suppl 8):3–5
18. Guo Y, Zhang C, Shang FF, Luo M, You Y, Zhai Q et al (2020) Ketogenic Diet Ameliorates Cardiac Dysfunction via Balancing Mitochondrial Dynamics and Inhibiting Apoptosis in Type 2 Diabetic Mice. Aging Dis 11(2):229–240
19. Bhanpuri NH, Hallberg SJ, Williams PT, McKenzie AL, Ballard KD, Campbell WW et al. Cardiovascular disease risk factor responses to a type 2 diabetes care model including nutritional ketosis induced by sustained carbohydrate restriction at 1 year: an open label, non-randomized, controlled study. Cardiovasc Diabetol. 2018;17
20. Chandrasekaran P, Rani PK. Reversal of diabetic tractional retinal detachment attributed to keto diet. BMJ Case Rep. 2020;13(10)
21. Barry D, Ellul S, Watters L, Lee D, Haluska R Jr, White R (2018) The ketogenic diet in disease and development. Int J Dev Neurosci 68:53–58
22. Yuan X, Wang J, Yang S, Gao M, Cao L, Li X et al (2020) Effect of the ketogenic diet on glycemic control, insulin resistance, and lipid metabolism in patients with T2DM: a systematic review and meta-analysis. Nutr Diabetes 10(1):38
23. Kumar S, Behl T, Sachdeva M, Sehgal A, Kumari S, Kumar A et al (2021) Implicating the effect of ketogenic diet as a preventive measure to obesity and diabetes mellitus. Life Sci 264:118661
24. Poplawski MM, Mastaitis JW, Isoda F, Grosjean F, Zheng F, Mobbs CV (2011) Reversal of diabetic nephropathy by a ketogenic diet. PLoS One 6(4):e18604
25. Puchalska P, Crawford PA (2017) Multi-dimensional Roles of Ketone Bodies in Fuel Metabolism, Signaling, and Therapeutics. Cell Metab 25(2):262–284

26. Newman JC, Verdin E (2014) Ketone bodies as signaling metabolites. Trends Endocrinol Metab 25(1):42–52
27. Uchihashi M, Hoshino A, Okawa Y, Ariyoshi M, Kaimoto S, Tateishi S et al. Cardiac-Specific Bdh1 Overexpression Ameliorates Oxidative Stress and Cardiac Remodeling in Pressure Overload-Induced Heart Failure. Circ Heart Fail. 2017;10(12)
28. Izuta Y, Imada T, Hisamura R, Oonishi E, Nakamura S, Inagaki E et al. Ketone body 3-hydroxybutyrate mimics calorie restriction via the Nrf2 activator, fumarate, in the retina. Aging Cell. 2018;17(1)
29. Torres JA, Kruger SL, Broderick C, Amarlkhagva T, Agrawal S, Dodam JR et al. Ketosis Ameliorates Renal Cyst Growth in Polycystic Kidney Disease. Cell Metab. 2019;30(6):1007–1023 e5
30. Xu H, Sun F, Li X, Sun L (2018) Down-regulation of miR-23a inhibits high glucose-induced EMT and renal fibrogenesis by up-regulation of SnoN. Hum Cell 31(1):22–32
31. Pascual G, Avgustinova A, Mejetta S, Martin M, Castellanos A, Attolini CS et al (2017) Targeting metastasis-initiating cells through the fatty acid receptor CD36. Nature 541(7635):41–45
32. Pfaffl MW (2001) A new mathematical model for relative quantification in real-time RT-PCR. Nucleic Acids Res 29(9):e45
33. Vidali S, Aminzadeh S, Lambert B, Rutherford T, Sperl W, Kofler B et al (2015) Mitochondria: The ketogenic diet–A metabolism-based therapy. Int J Biochem Cell Biol 63:55–59
34. Paoli A, Rubini A, Volek JS, Grimaldi KA (2013) Beyond weight loss: a review of the therapeutic uses of very-low-carbohydrate (ketogenic) diets. Eur J Clin Nutr 67(8):789–796
35. Elmarakby AA, Sullivan JC (2012) Relationship between oxidative stress and inflammatory cytokines in diabetic nephropathy. Cardiovasc Ther 30(1):49–59
36. Ha H, Hwang IA, Park JH, Lee HB (2008) Role of reactive oxygen species in the pathogenesis of diabetic nephropathy. Diabetes Res Clin Pract 82(Suppl 1):S42–S45
37. Mittal M, Siddiqui MR, Tran K, Reddy SP, Malik AB (2014) Reactive oxygen species in inflammation and tissue injury. Antioxid Redox Signal 20(7):1126–1167
38. Brownlee M (2005) The pathobiology of diabetic complications: a unifying mechanism. Diabetes 54(6):1615–1625
39. Zhang DD (2006) Mechanistic studies of the Nrf2-Keap1 signaling pathway. Drug Metab Rev 38(4):769–789
40. Nezu M, Suzuki N, Yamamoto M (2017) Targeting the KEAP1-NRF2 System to Prevent Kidney Disease Progression. Am J Nephrol 45(6):473–483
41. Wang D, Tai PWL, Gao G (2019) Adeno-associated virus vector as a platform for gene therapy delivery. Nat Rev Drug Discov 18(5):358–378
42. Kuzmin DA, Shutova MV, Johnston NR, Smith OP, Fedorin VV, Kukushkin YS et al (2021) The clinical landscape for AAV gene therapies. Nat Rev Drug Discov 20(3):173–174
43. Chen BD, He CH, Chen XC, Pan S, Liu F, Ma X et al (2015) Targeting transgene to the heart and liver with AAV9 by different promoters. Clin Exp Pharmacol Physiol 42(10):1108–1117

44. Zhao L, Gao H, Lian F, Liu X, Zhao Y, Lin D (2011) (1)H-NMR-based metabonomic analysis of metabolic profiling in diabetic nephropathy rats induced by streptozotocin. Am J Physiol Renal Physiol 300(4):F947–F956
45. Zhang Q, Shen F, Shen W, Xia J, Wang J, Zhao Y et al (2020) High-Intensity Interval Training Attenuates Ketogenic Diet-Induced Liver Fibrosis in Type 2 Diabetic Mice by Ameliorating TGF-beta1/Smad Signaling. Diabetes Metab Syndr Obes 13:4209–4219
46. Ko GJ, Rhee CM, Kalantar-Zadeh K, Joshi S (2020) The Effects of High-Protein Diets on Kidney Health and Longevity. J Am Soc Nephrol 31(8):1667–1679

Figures

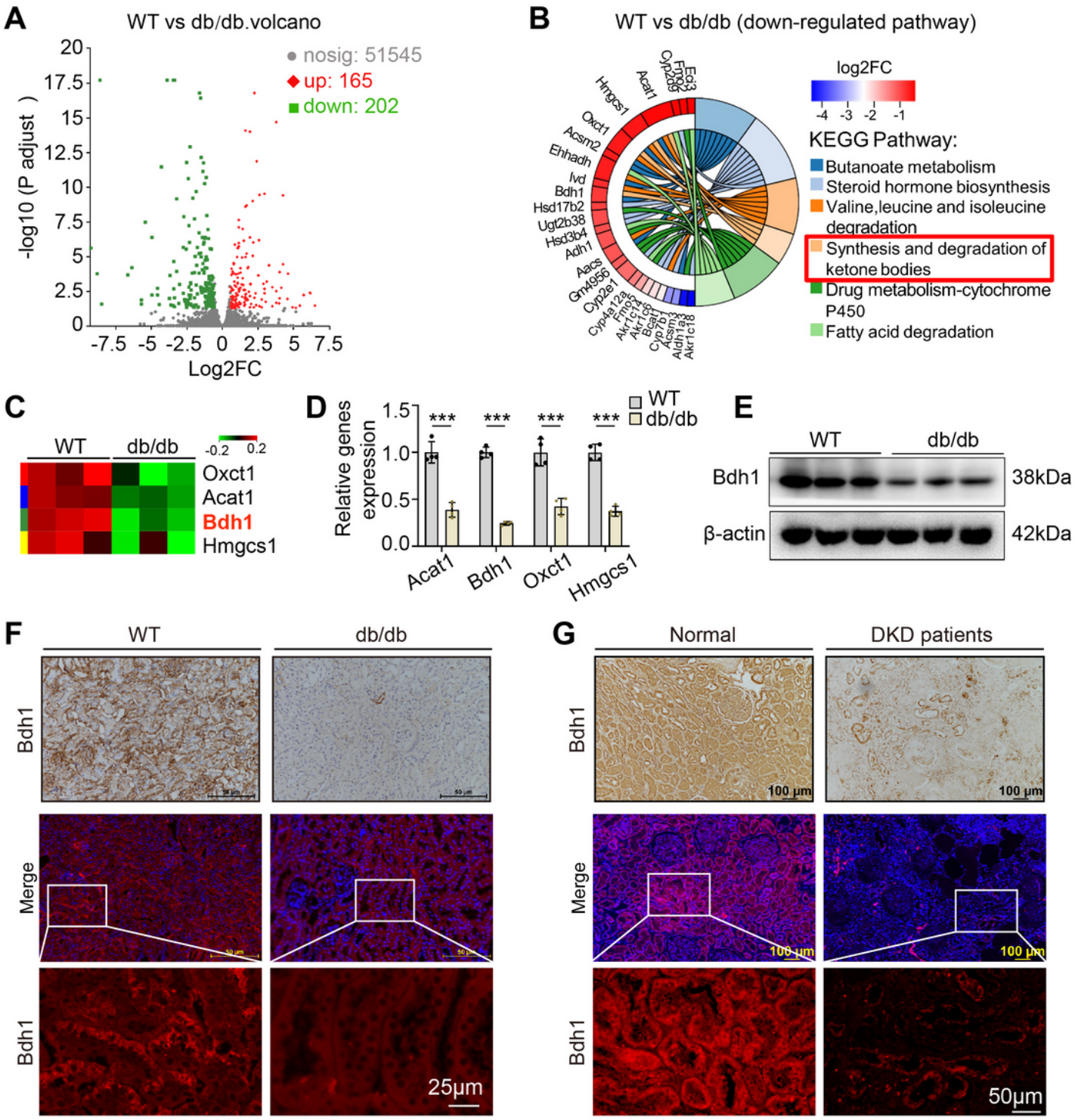

Figure 1

Bdh1 expression is down-regulated in diabetic kidneys. (A) A volcano plot showing DEGs (red, upregulated genes; green, downregulated genes) in kidneys from WT and db/db mice (n=3 mice per group). (B) KEGG enrichment analysis showing the top 6 down-regulated pathways. (C) The four differentially expressed genes involved in the pathway of synthesis and degradation of ketone bodies. (D) qRT-PCR analysis showing the mRNA levels of Acat1, Bdh1, Oxct1 and Hmgcs1 in kidneys from WT and

db/db mice (n=3 mice per group). WB (E), IHC and IF (F) showing the protein level of Bdh1 in kidneys from WT and db/db mice. IHC and IF(G) showing the protein level of Bdh1 in kidneys from normal subjects (n=9) and patients with DKD (n=8). All results are representative of three independent experiments. Values are presented as mean ± SD. Bar: 50μm and 25μm in F, 100μm and 50μm in G. ***P <0.001.

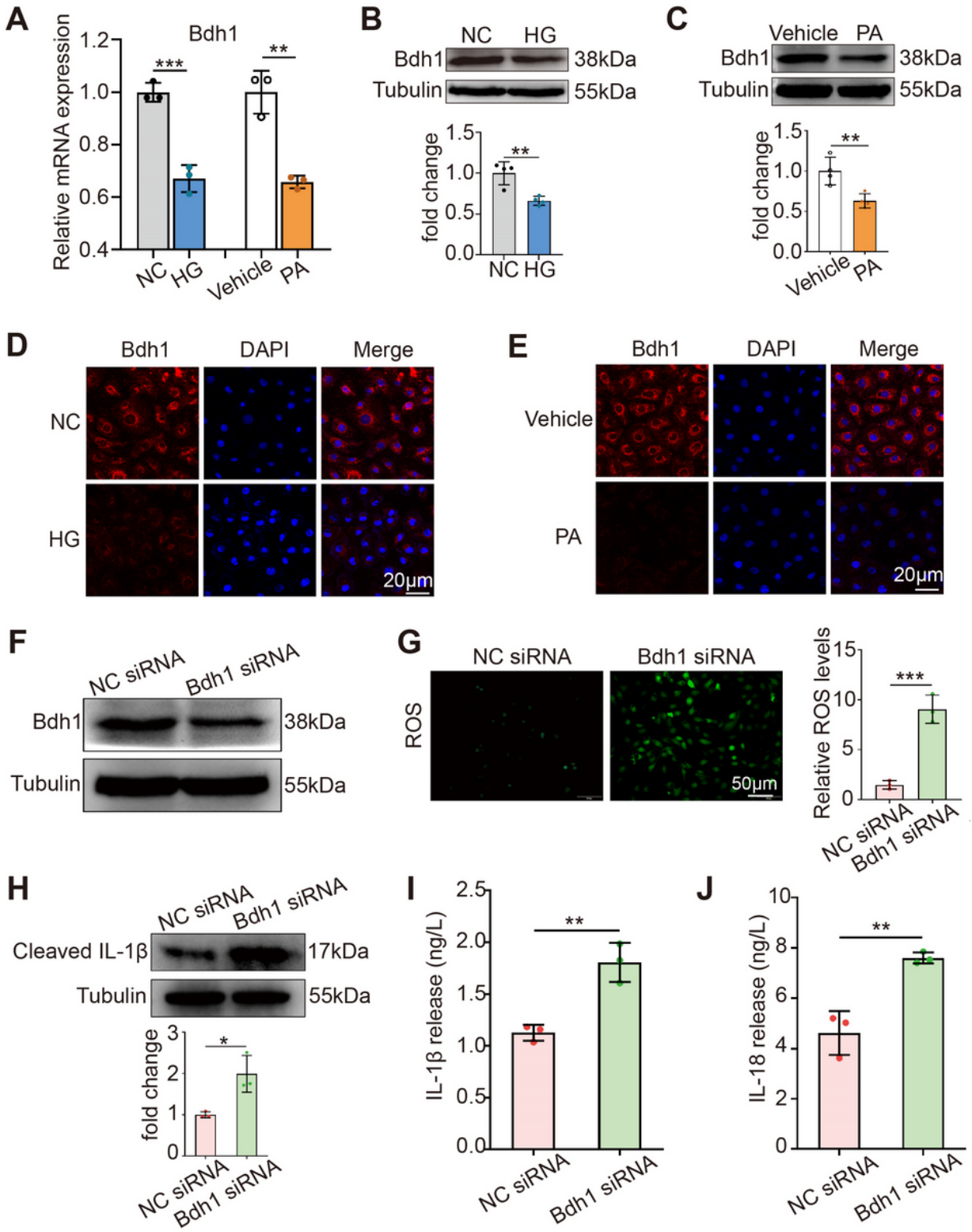

Figure 2

Bdh1 deficiency mediated HG or PA-induced increase of ROS and proinflammatory cytokines in HK-2 cells. (A) qRT-PCR showing the mRNA level of Bdh1 in HK-2 cells treated with HG or PA. Representative WB images showing the protein level of Bdh1 in HK-2 cells stimulated by HG (B) or PA (C). Representative IF images showing the protein level of Bdh1 in HK-2 cells stimulated by HG (D) or PA (E). Bar: 20μm. (F) Representative WB image showing the protein level of Bdh1 in HK-2 cells transfected with normal control (NC) siRNA or Bdh1 siRNA. (G) DCFH-DA probe was used to detect the level of ROS in HK-2 cells transfected with NC siRNA or Bdh1 siRNA. Bar: 50μm. (H) Representative WB image showing the protein level of IL-1β in HK-2 cells transfected with NC siRNA or Bdh1 siRNA. (I-J) ELISA assay showing the levels of IL-1β (I) and IL-18 (J) in cell culture supernatant of HK-2 cells transfected with NC siRNA or Bdh1 siRNA. All results are representative of three independent experiments. Values are presented as mean ± SD. *P<0.05; **P<0.01; ***P<0.001.

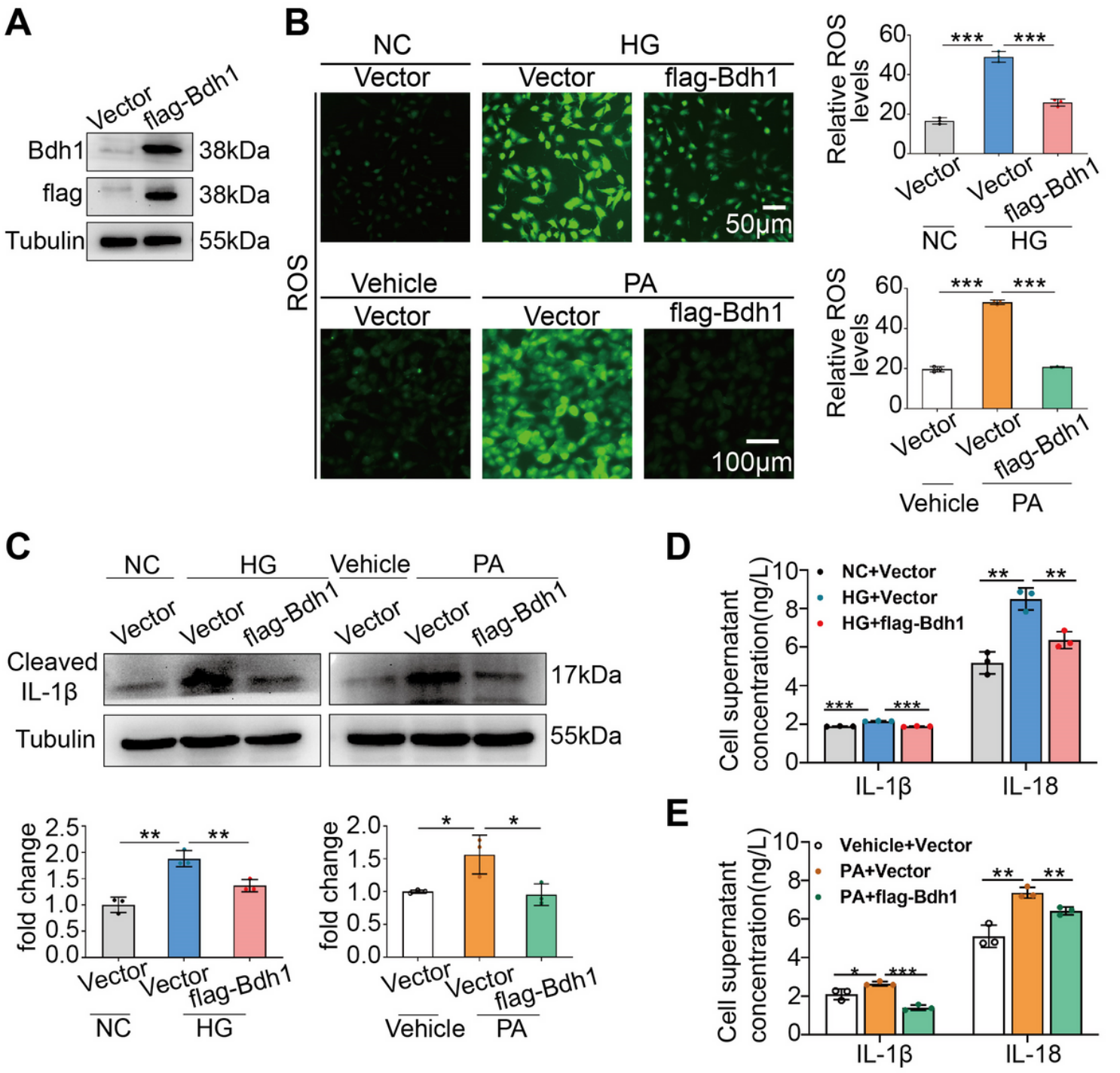

Figure 3

Bdh1 overexpression reversed HG or PA-induced increase of ROS and proinflammatory cytokines. (A) Representative WB image showing the protein level of Bdh1 in HK-2 cells transfected with vector or flag-Bdh1. (B) DCFH-DA probe was used to detect the level of ROS in HK-2 cells with indicated treatment. Bar: 50μm in upper panels and 100μm in lower panels. (C) Representative WB image showing the protein level of IL-1β in HK-2 cells with indicated treatment. (D-E) ELISA assay showing the levels of IL-1β and IL-18 in the cell culture supernatant of Bdh1-overexpressed HK-2 cells treated by HG (D) or PA (E). For samples used in B-E, HK-2 cells were transfected with the plasmids overexpressing flag-Bdh1 or vector for 6h, and

then treated with HG or PA for 48h. All results are representative of three independent experiments. Values are presented as mean ± SD. *P<0.05; **P<0.01; ***P<0.001.

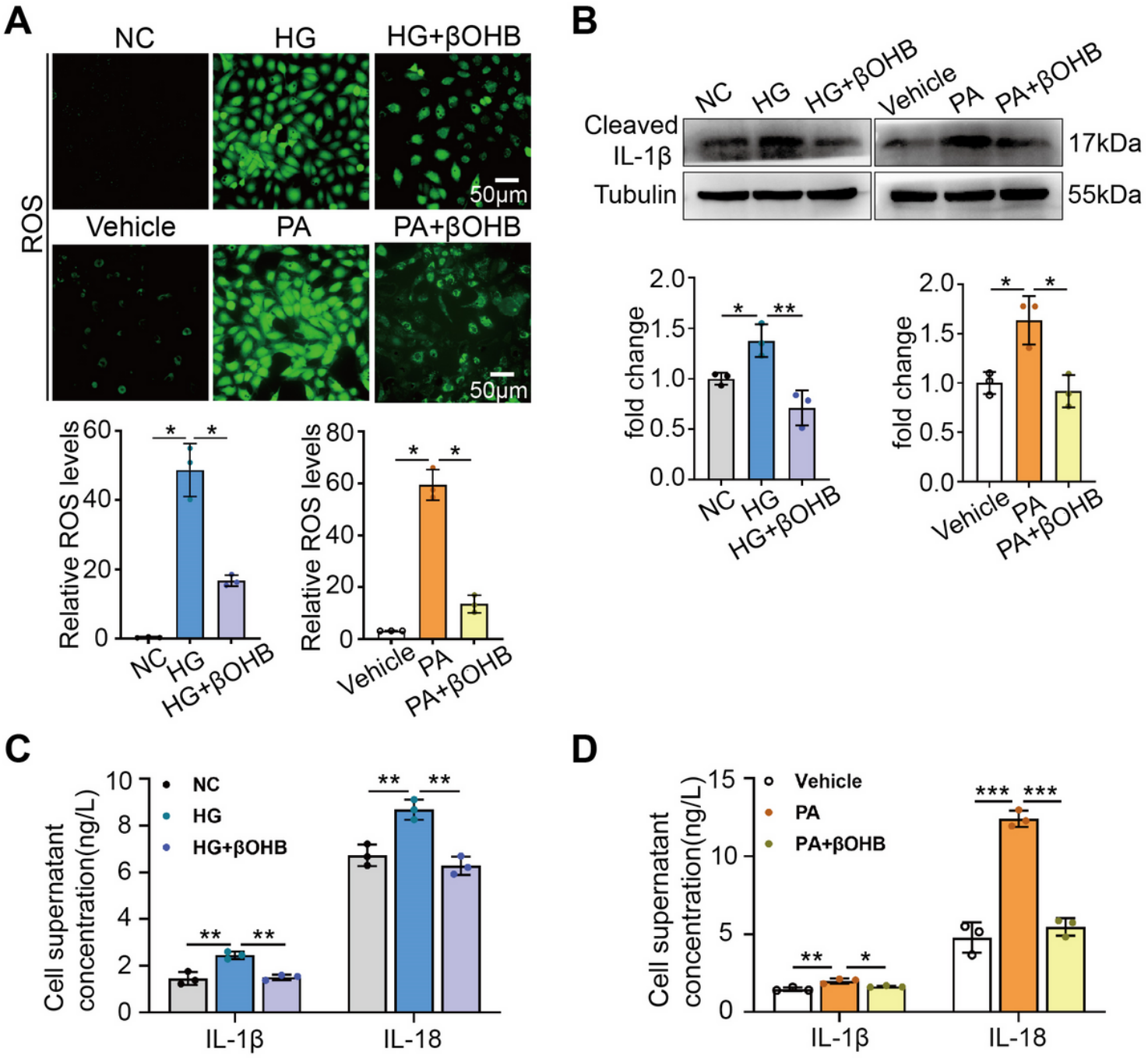

Figure 4

βOHB supplementation reversed HG or PA-induced increase of ROS and proinflammatory cytokines. (A) DCFH-DA probe was used to detect ROS levels in HK-2 cells with indicated treatment. Bar: 50μm. (B) Representative WB image showing the protein level of IL-1β in HK-2 cells with indicated treatment. (C-D) ELISA assay showing the levels of IL-1β and IL-18 in the cell culture supernatant of βOHB-supplied HK-2 cells treated by HG (C) or PA (D). For samples used in A-D, HK-2 cells were respectively treated with vehicle or βOHB and HG or PA for 48h. All results are representative of three independent experiments. Values are presented as mean ± SD. *P<0.05; **P<0.01; ***P<0.001.

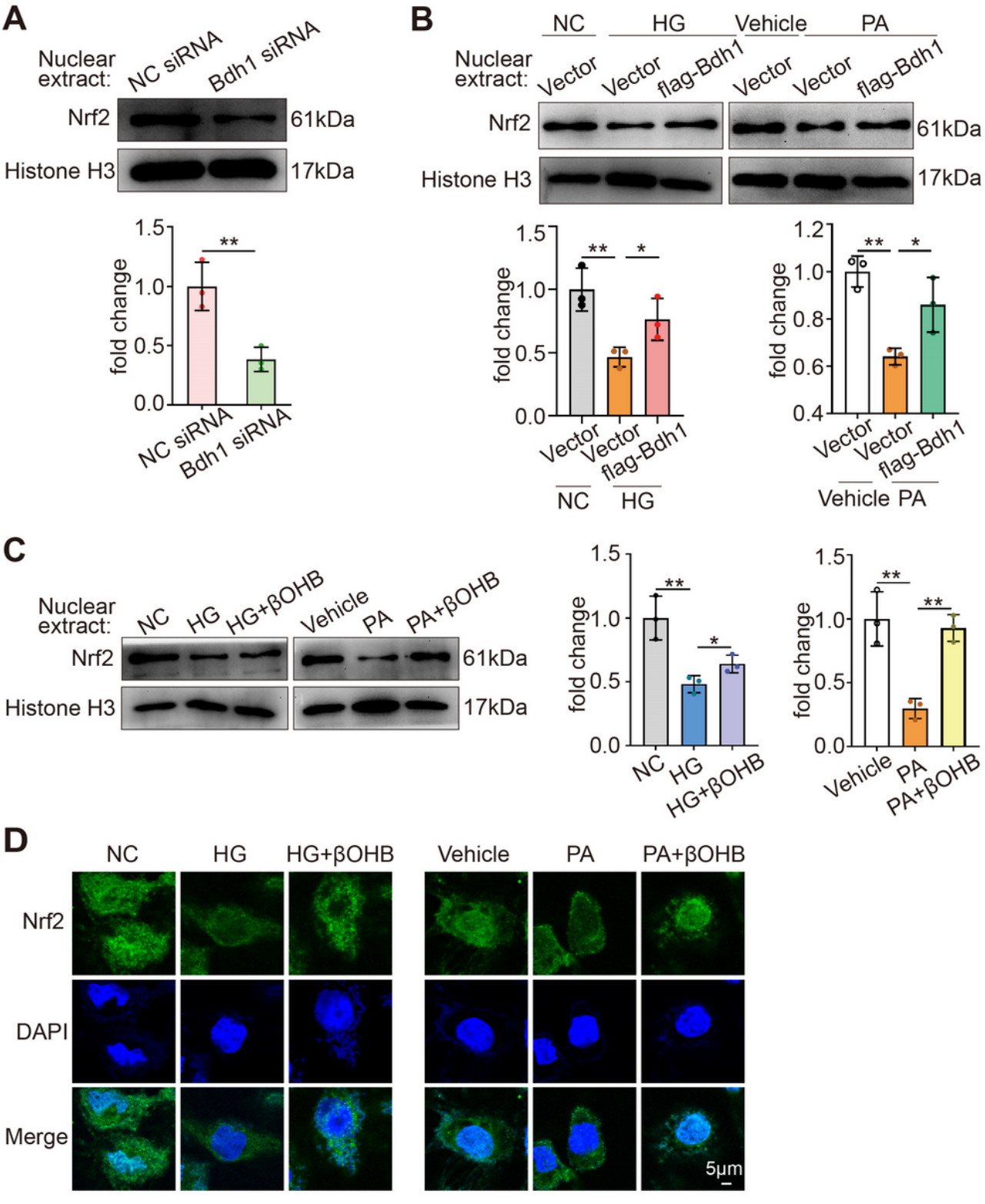

Figure 5

Bdh1 mediated βOHB metabolism promoted Nrf-2 nuclear translocation. (A) Representative WB image showing the protein level of Nrf2 protein in the nuclear of HK-2 cells transfected with NC siRNA or Bdh1 siRNA. (B) Representative WB images showing the protein level of Nrf2 in the nuclear of Bdh1-overexpressed HK-2 cells treated by HG or PA. (C) Representative WB images showing the protein level of Nrf2 in the nuclear of βOHB-supplied HK-2 cells treated by HG or PA. (D) Representative IF images

showing the location of Nrf2 in βOHB-supplied HK-2 cells treated by HG or PA. Bar: 5μm. All results are representative of three independent experiments. Values are presented as mean ± SD. *P<0.05; **P<0.01.

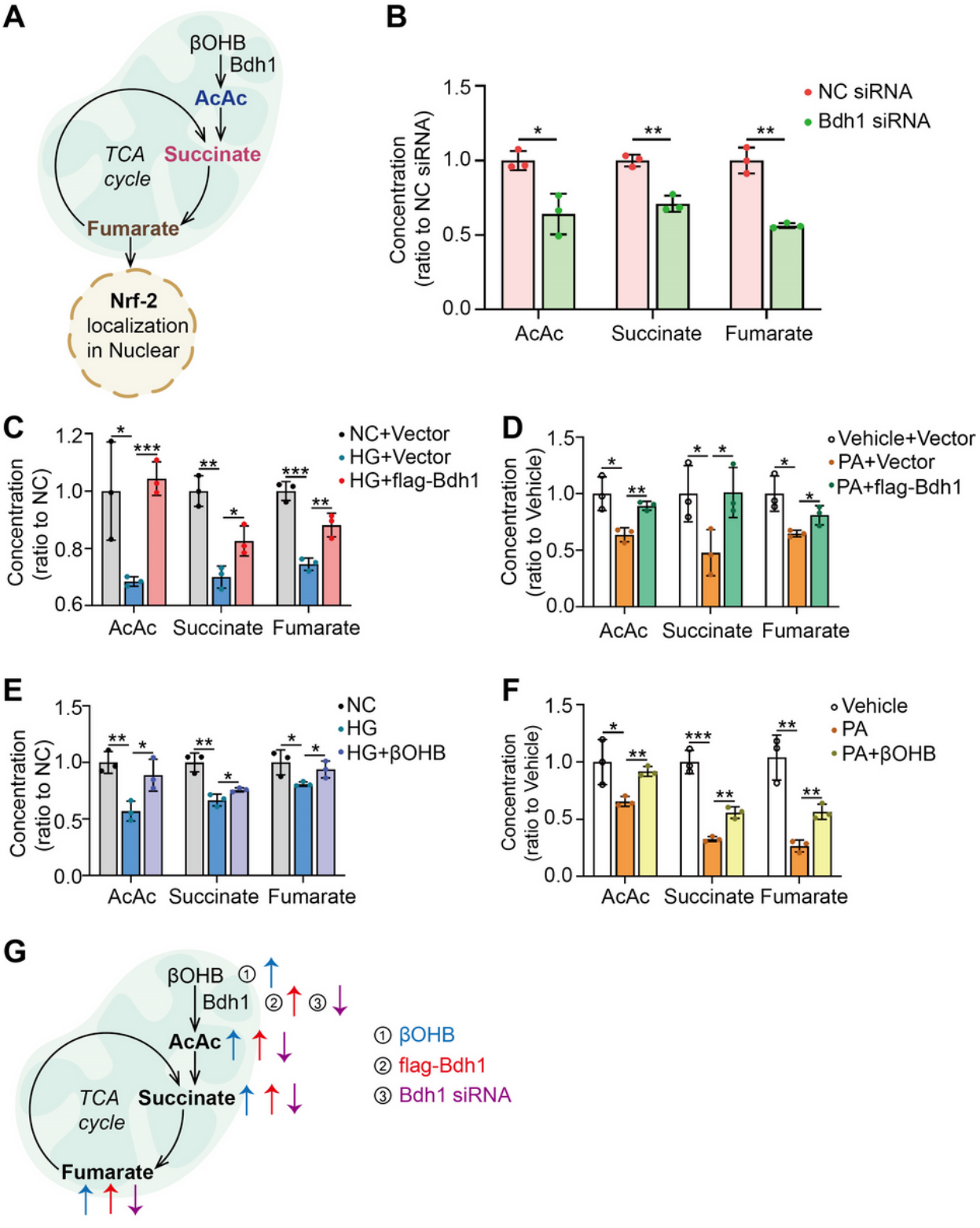

Figure 6

Bdh1-mediated βOHB metabolism promoted the fumarate production through AcAc-succinate-fumarate metabolic pathway. (A) Scheme showing the connections among Bdh1 mediated βOHB metabolism, TCA cycle and Nrf2. (B) The concentrations of AcAc, succinate and fumarate in HK-2 cells transfected with NC

siRNA or Bdh1 siRNA. (C-D) The concentrations of AcAc, succinate and fumarate in Bdh1 overexpressed HK-2 cells stimulated by HG (C) or PA (D). (E-F) The concentrations of AcAc, succinate and fumarate in βOHB-supplied HK-2 cells stimulated by HG (E) or PA (F). (G) Scheme showing the Bdh1-regulated metabolic flux composed of βOHB-AcAc-succinate-fumarate. All results are representative of three independent experiments. Values are presented as mean ± SD. *P<0.05; **P<0.01; ***P<0.001.

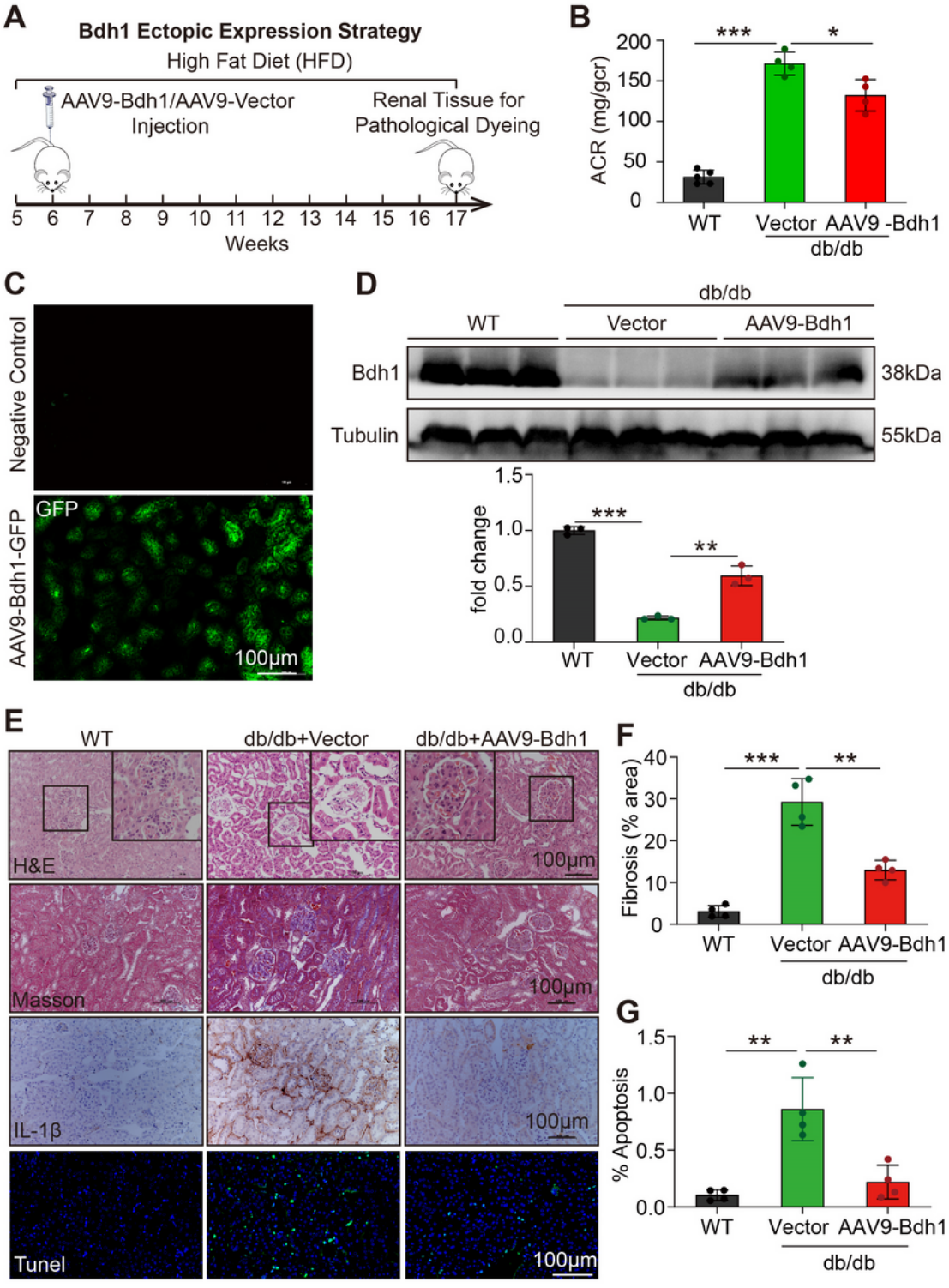

Figure 7

AAV9-mediated Bdh1 ectopic expression in kidney alleviated the progression of DKD. (A) A schematic representation of the Bdh1 ectopic expression strategy in db/db mice. (B) Urinary ACR values of mice in indicated group (n=5 in WT group, n=4 in AAV-vector and AAV-Bdh1 injected db/db group). (C) Representative renal fluorescent images of the mice 12 weeks after caudal vein delivery of AAV-Bdh1 encoding green fluorescent protein (GFP) demonstrating the GFP expression in the kidney. (D) Representative WB image showing the protein level of Bdh1 in kidneys from indicated groups. (E) The representative photomicrographs of H&E, Masson, IHC(IL-1β) and Tunel staining showing the pathological changes in kidneys from indicated groups. Bar: 100μm. (F) Quantification of the fibrosis area in kidneys from indicated groups (n=4 per group). (G) Quantification of apoptosis positive cells in kidneys from indicated groups (n=4 per group). All results are representative of three independent experiments. Values are presented as mean ± SD. ACR: Albumin-Creatinine Ratio. *p<0.05; **p<0.01; ***p<0.001.

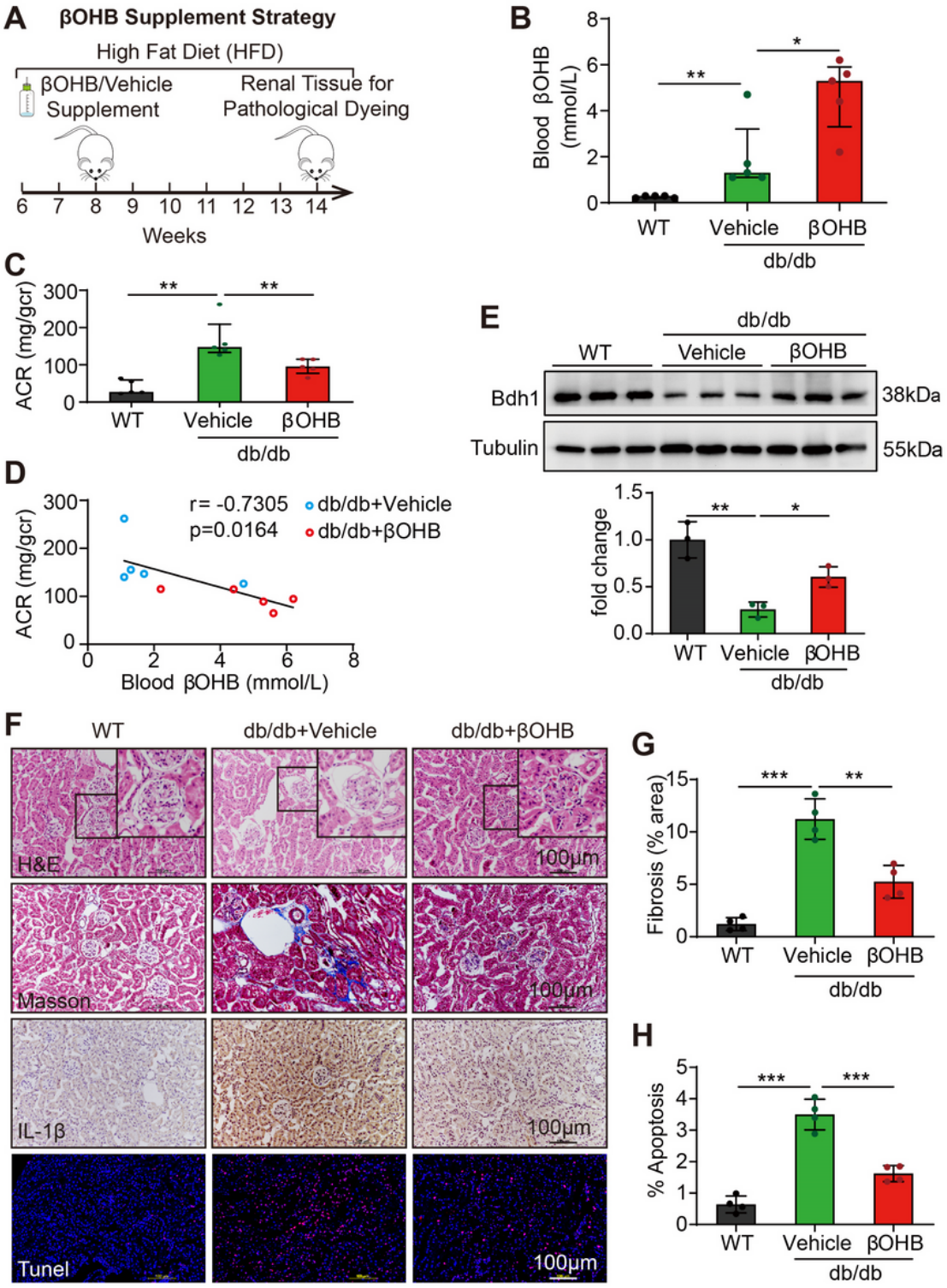

Figure 8

βOHB Supplementation alleviated the progression of DKD. (A) A schematic representation of the βOHB intervention strategy in db/db mice. (B) Blood level of βOHB in mice from indicated groups (n=5 per group). (C) Urinary ACR values of mice from indicated groups (n=5 per group). (D) Negative correlation between serum βOHB level and ACR in db/db mice with vehical and βOHB treatment. (E) Representative WB image showing the protein level of Bdh1 in kidneys from indicated groups. (F) The representative

photomicrographs of H&E, Masson, IHC(IL-1β) and Tunel staining showing the pathological changes in kidneys from indicated groups. Bar: 100μm. (G) Quantification of the fibrosis area in kidneys from indicated groups (n=4 per group). (H) Quantification of apoptosis positive cells in kidneys from indicated groups (n=4 per group). All results are representative of three independent experiments. Values are presented as mean ±SD. ACR: Albumin-Creatinine Ratio; *p<0.05; **p<0.01; ***p<0.001.

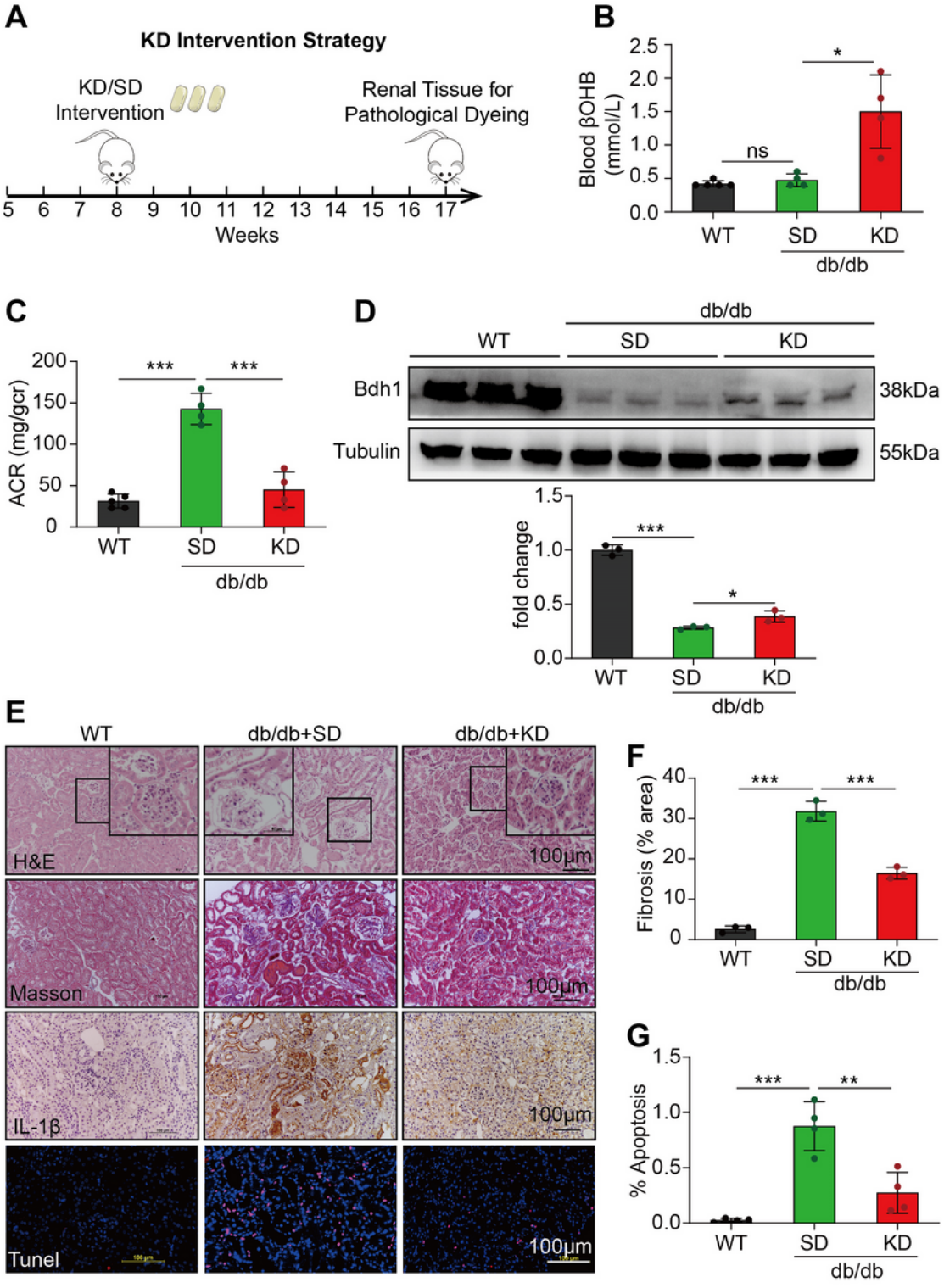

Figure 9

The ketogenic diet alleviated the progression of DKD. (A) A schematic representation of the KD intervention strategy in db/db mice. (B) Blood level of βOHB in mice from indicated groups (n=5 in WT group; n=4 in SD and KD group). (C) Urinary ACR values of mice in indicated groups (n=5 in WT group, n=4 in SD and KD group). (D)Representative WB image showing the protein level of Bdh1 in kidneys from indicated groups. (E) The representative photomicrographs of H&E, Masson, IHC(IL-1β) and Tunel staining showing the pathological changes in kidneys from indicated groups. Bar: 100μm. (F) Quantification of the fibrosis area in kidneys from indicated groups (n=4 per group). (G) Quantification of apoptosis positive cells in kidneys from indicated groups (n=4 per group). All results are representative of three independent experiments. Values are presented as mean ± SD. ACR: Albumin-Creatinine Ratio; SD: Standard Diet; KD: Ketogenic Diet; ns: no significance; *p<0.05; **p<0.01; ***p<0.001.

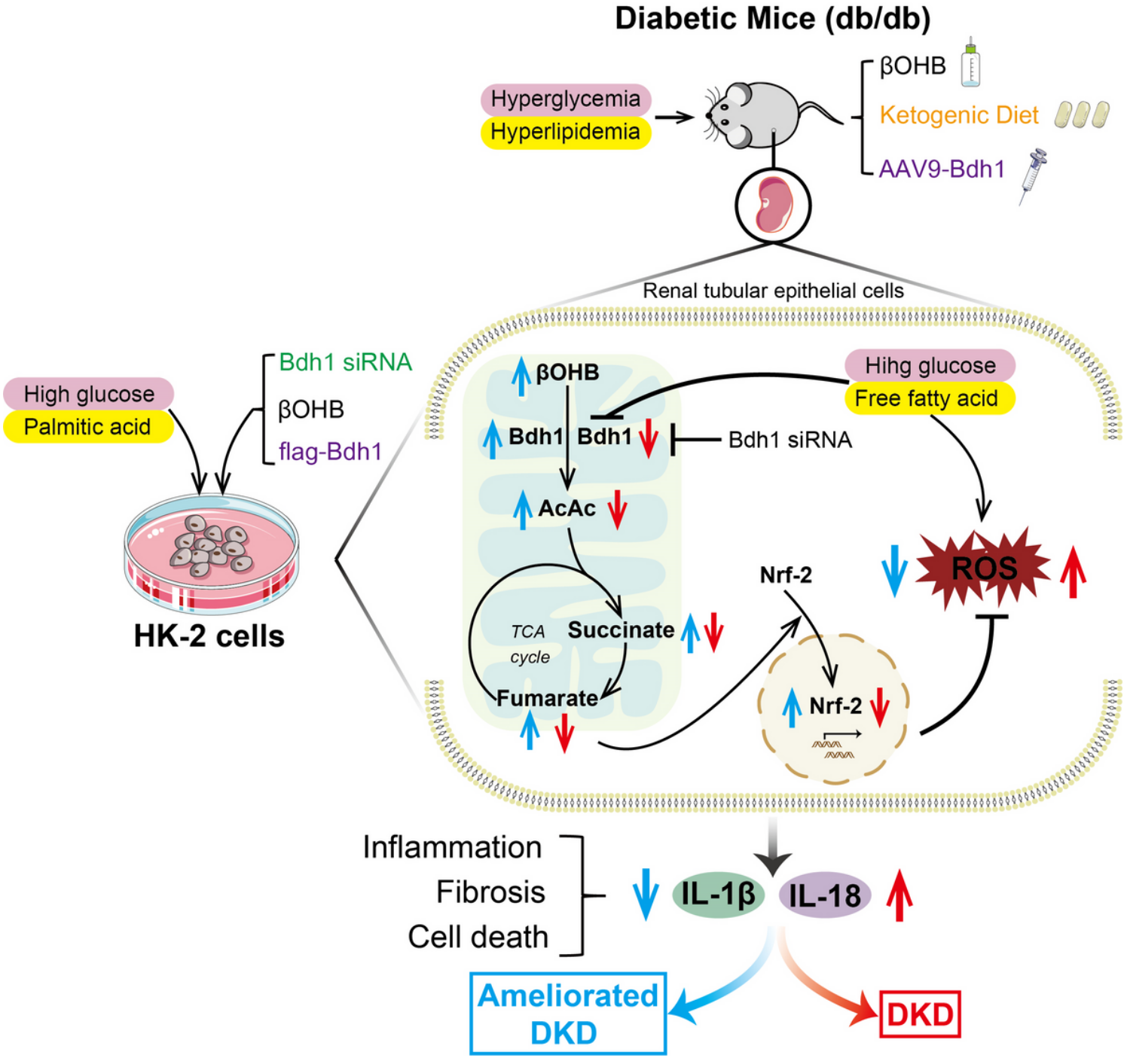

Figure 10

Schematic diagram depicting the mechanism by which Bdh1-mediated βOHB metabolism ameliorates DKD.

Supplementary Files

This is a list of supplementary files associated with this preprint. Click to download.

- Supplementaryfiles.pdf
- Supplementarymaterials.docx
- Supplementarytable2.xls